Inorganic Chemistry Research

Article

Cu_2O/AlZn-LDH Preparation on FTO Electrode Substrate for Enhanced Water Oxidation

Karim Asadpour-Zeynali[a,*], Parisa Beikzadeh[a], Leila Jafari Foruzin[b] and Kamellia Nejati[c,*]

[a]*Department of Analytical Chemistry, Faculty of Chemistry, University of Tabriz, Tabriz, Iran*
[b]*Department of Chemistry, Faculty of Basic Sciences, Azarbaijan Shahid Madani University, P.O. Box: 53714-161, Tabriz, Iran*
[c]*Department of Chemistry, Payame Noor University, P.O. Box: 19395-3697, Tehran, Iran*

Received: July 11, 2021; Accepted: September 26, 2021
Cite This: *Inorg. Chem. Res.* **2021,** *5*, 239-245. DOI: 10.22036/icr.2021.294592.1110

Abstract: The electrochemical activity of the Cu_2O/AlZn-LDH, deposited on the FTO electrode, was investigated in NaOH (0.1 M) media. The thin film Cu_2O/AlZn-LDH was characterized by techniques such as X-ray diffraction (XRD), scanning electron microscopy (SEM), and energy-dispersive X-ray spectroscopy (EDX). Based on the obtained results from XRD, Cu_2O/AlZn-LDH was prepared in the nanometer size with good crystalline quality. The SEM images were shown the synthesis of a thin film Cu_2O/AlZn-LDH nanocomposite on the FTO electrode. The water oxidation results show that Cu_2O-Zn/Al-LDH modified FTO electrode is an improved electrocatalyst and has high activity at water oxidation in alkaline media with the onset potential about 0.6 V vs. SCE and overpotential of 380 mV at10 mA/cm. The improved water oxidation activity at Cu_2O/AlZn-LDH can be attributed to the good conductivity of the nanocomposite.

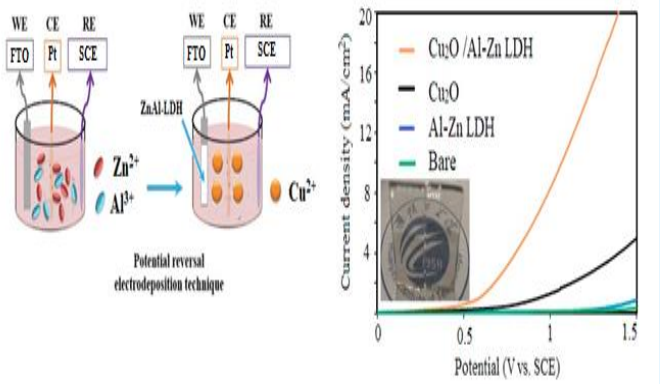

Keywords: Electrocatalyst, Layered Double Hydroxide (LDH), FTO Electrode, Oxygen evolution reaction (OER)

1. INTRODUCTION

In recent years, in order to obtain clean energy, the electrochemical water oxidation has been increasingly studied.[1-5] Among all the researches, the oxygen evolution reaction (OER) using electrocatalysts is considered as a key issue at water oxidation. In this process, four-electrons are transferred in an anodic reaction.[6-10] In the recent years, various metal electrocatalysts such as oxides,[11-13] phosphides[14-17] and hydroxides[18, 19] have been applied as new materials for water oxidation. The oxygen generation process is kinetically sluggish, because at water oxidation, potential about 1.23 V is needed due to multistep proton-coupled electron transfer (PCET).[20, 21] The water oxidation reaction in base or acidic solution is occurred as follows:

$$4OH^- \rightarrow 2H_2O + O_2 + 4e^- \text{ base solution} \quad (1)$$

$$2H_2O \rightarrow 4H^+ + O_2 + 4e^- \text{ acidic solution} \quad (2)$$

The first-row transition metal electrocatalysts in forms such as nanocomposites,[22-26] perovskites,[27] and layered double hydroxides,[28-30] with high activity have been comprehensively studied. In the recent years, important studies on improving of LDH-based materials have been reported. In 2015, Dai et al. published a mini-review for water oxidation using NiFe-based electrocatalysts,[31] where the applications and related mechanisms have been bringing up briefly. Shao et al. reported the improvement of Layered based materials for energy conversion using electrocatalysts.[32] In the mentioned study, the applications of water oxidation have been discussed. Also, a review article was published by Strasser et. al. which was focused on the development of NiFe-based materials.[33] Other privileged researches have been reported LDH-based materials for water oxidation, including the design of electrocatalyst oxides and hydroxides of transition metal by Boettcher et al.[34]

Layered double hydroxides (LDHs), are a family of anionic clays. In these materials the general formula is reported as $[M^{II}_{1-X}M_x(OH)_2]^{x+}$ $[A^{n-}_{x/n}\cdot yH_2O]^{x-}$, where M^{III} and M^{II} represent trivalent and divalent metal ions, respectively, and A^{n-} is defined as an anion with n^- valent. The LDH layers consist positive charge due to partial substitution of M^{II} by M^{III}. This positive charge was neutralized using anions which intercalated at the interlayer of LDHs.[35] Transition metal based LDHs, have

received considerable attention due to their potential efficiency in catalysis, adsorbents, drug delivery, anion exchangers, biotechnology, photoactive materials, electrochemistry, nanocomposites, magnetization, and environmental applications. Also, the LDHs have some interesting properties, such as simple and economical synthesis in the laboratory and industrial scales with properties such as nanoscale size, specific structure, improved chemical composition, large surface areas, variable layer charge density, colloidal properties, flexible tunability, swelling in water, good thermal stability, etc.[36] Synthesis of LDHs on the FTO was interested at last years. FTO coated glasses have many advantages; example being: thigh electrical conductivity, good thermal and mechanical resistance, providing in any dimensions necessary, reasonably priced, and using in photo-electronic and photovoltaic devices. They are stable in different environmental conditions and also are chemically inert.

In the present work, Cu_2O/AlZn-LDH was prepared using the simple electrodeposition method on the FTO electrode. The obtained nanocomposite was then applied as electrocatalysts at water oxidation in 0.1 M KOH with high activity and small overpotential.

2. EXPERIMENTAL

Apparatus and software

Electrochemical investigations were achieved using a Sama 500 Electrochemical Analysis System (Sama, Iran) interfaced with a personal computer (PC) and a three-electrode configuration. FTO electrode modified with Cu_2O/AlZn-LDH was applied as the working electrode. A saturated calomel electrode and a Pt wire were utilized as the reference and counter electrodes, respectively (the working, counter, and reference electrodes were obtained from Azar Electrode Co, Urmia, Iran). The pH measurements were carried out using a Metrohm pH-meter 691. All the measurements were carried out at room temperature (25 ± 0.5 °C). The X-ray diffraction (XRD) patterns were collected with a Bruker AXS model D8 Advance diffractometer using Cu-K_α radiation (λ = 1.542 Å), with the Bragg angle of 2-70°, performing steps of 0.04°(2θ), and counting 4 s/step. The scanning electron microscopy (SEM)/energy dispersive X-ray (EDX) analysis was performed using a MIRA3 TESCAN scanning electron microscope equipped with an EDX system. The accelerating voltage was 10 kV, with a beam current of 1 nA and a spectrum collection time of 100 s. The FT-IR spectra were recorded on a Bruker tensor 27 spectrometer.

Reagents and solutions

$Zn(NO_3)_2.6H_2O$, $Al(NO_3)_3.9H_2O$ and $CuSO_4.5H_2O$ were applied without further purification and were prepared from Merck Company. Citric acid (0.960 g) and $CuSO_4.5H_2O$ (1.248 g) were solved in 100 mL of deionized water for preparation of a 0.05 M solution contain citric acid ($C_6H_8O_7$) and copper sulfate ($CuSO_4$). Also, KCl (0.187 g), $[Fe(CN)_6]^{3-}$ (0.008 g) and $[Fe(CN)_6]^{4-}$ (0.010 g) were solved in deionized water (25 mL) to prepare solutions contain KCl (0.1 M), and (0.5 mM) $[Fe(CN)_6^{3-}$ and $Fe(CN)_6^{4-}]$.

Fabrication of modified electrode

For the preparation of AlZn-LDH, the FTO electrode (0/5 cm × 0/5 cm) was first immersed in an electrochemical cell containing 15 mM $Zn(NO_3)_2.6H_2O$ (as the Zn^{2+} source) and 5 mM $Al(NO_3)_3.9H_2O$ (as the Al^{3+} source) solution. Then AlZn-LDH was deposited on the surface of the FTO electrode as thin film by applying a potential of -1.65 V/SCE for 120 s using the electro-deposition method.

For the synthesis of Cu_2O/AlZn-LDH, the prepared AlZn-LDH electrode was immersed in an electrochemical cell containing 0.05 M $CuSO_4$ and 0.05 M citric acid solution and nanocomposite was synthesized by chronoamperometry method at potential of -0.5 V for 180 s at the 65 °C. Then the prepared electrode was kept at temperature 80 °C for 2 h.

3. RESULTS AND DISCUSSION

X-ray diffraction

The XRD patterns of AlZn-LDH and AlZn-LDH/Cu_2O nanoparticles are shown in Figure 1(a) and (b). The X-ray diffraction pattern of the AlZn-LDH synthesized on the FTO electrode is shown in Figure 1(a). The sharp and strong diffractions at 2θ = 9.91° and 19.78°, are related to plates of (003) and (006) at layered double hydroxide, respectively, and also the diffraction in the 2θ = 33.68 ° is related to ZnO (002) plate. Comparison with the reference diffraction pattern indicates that the pattern is completely consistent with the pattern obtained by other researchers and does not contain any impurities.[37] As can be seen, sharp diffractions in 2θ are equal to 33.46° and 43.12°

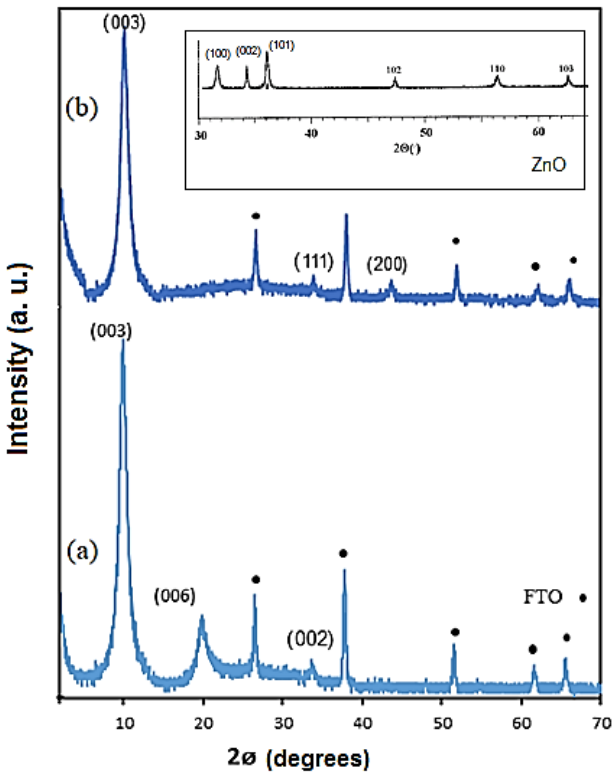

Figure 1. XRD patterns of (a) AlZn-LDH, and (b) Cu_2O/AlZn-LDH.

correspond to the plants of (111) and (200) at Cu_2O. Also, the sharp diffractions in the 2θ about 26.29°, 37.55°, 51.31°, 61.40°, and 65.33° are related to the FTO electrode.[38] The obtained results are consistent with the reported results by other researchers.[39] Also, the sharp and strong diffractions in region 2θ are equal to 9.91° are related to (003) LDH plate. The reported patterns indicate that the synthesized sample has a layered double hydroxide crystal structure and completely is composited with Cu_2O.

SEM image

SEM images of Cu_2O/AlZn-LDH coating on the FTO electrode with two different magnifications are shown in Figure 2(a) and (b). The synthesized compound consists of spherical nanoparticles that are stacked together.

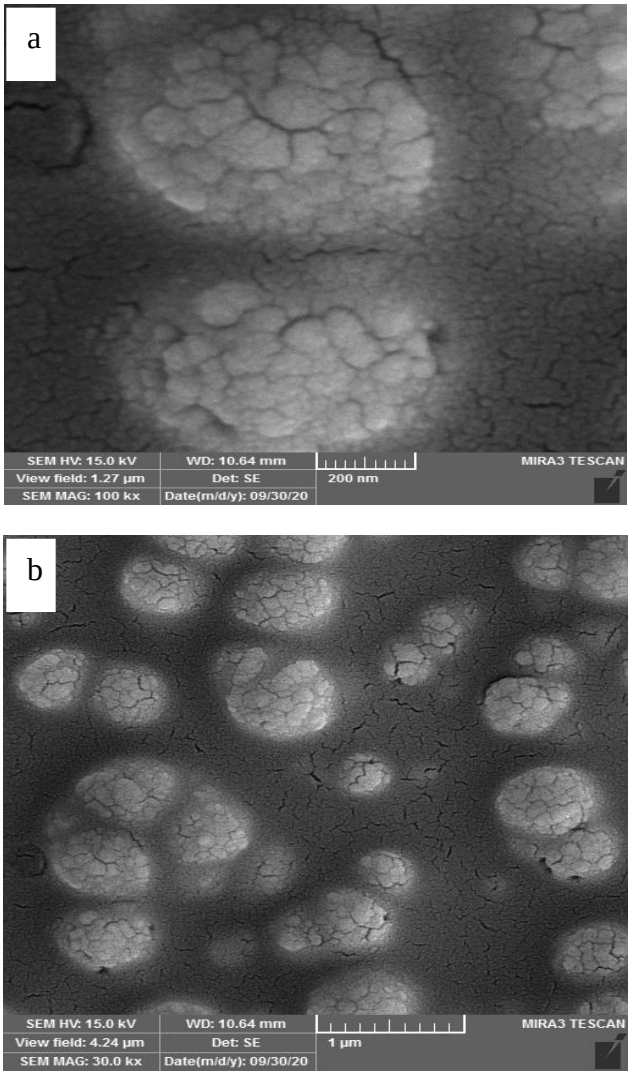

Figure 2. (a) and (b) SEM image of Cu_2O/AlZn-LDH at two different magnifications.

The obtained SEM images show the synthesis of Cu_2O/AlZn-LDH with the uniformity and homogeny nanoparticles on the surface of the FTO electrode. According to SEM images, particle sizes are estimated between 20 and 30 nanometers.

EDX (Energy-dispersive X-ray spectroscopy) and elemental map analysis

EDX analysis was reported in Figure 3 to investigate the chemical elemental of the synthesized Cu_2O/AlZn-LDH. The resulting EDX spectrum shows the existing peaks of the aluminum and zinc cations in the LDH. Also, the peaks of copper and oxygen atoms related to Cu_2O in Cu_2O/AlZn-LDH compound are also observed. The intensity of oxygen peak is low because the oxygen atom is lighter than Cu, Al and Zn atoms, so other relaxation processes may compete with the EDX. In addition, the presence of tin peaks, are related to the FTO electrode. The Au peak is also appeared due to covering the surface of the material with gold, for SEM imaging.

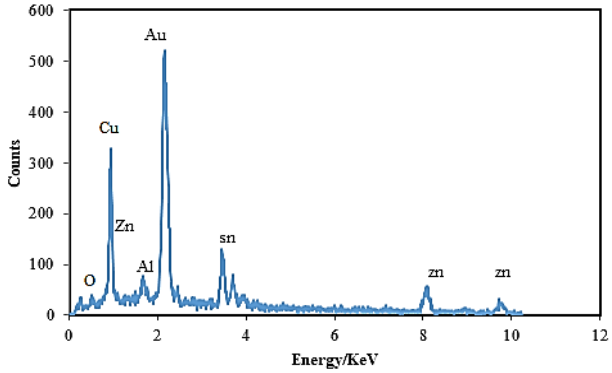

Figure 3. EDX spectrum of Cu_2O/AlZn-LDH.

The elemental map was used to investigate the distribution of Cu_2O/AlZn-LDH synthesized on the FTO electrode. Figure 4 confirmed the presence of Zn, O, Al,

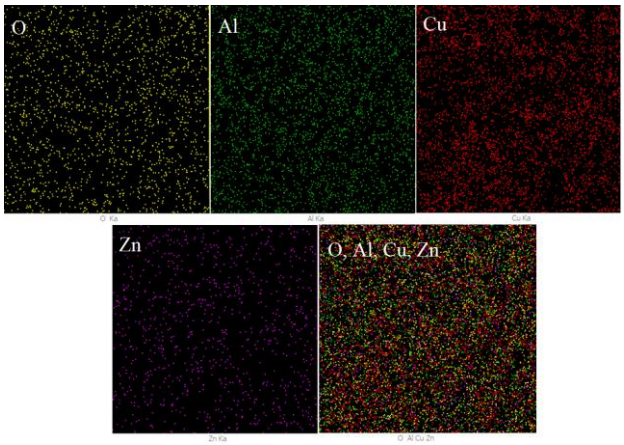

Figure 4. The elemental map of Cu_2O/AlZn-LDH.

and Cu elements in the prepared composite. Based on this distribution map, we conclude that the synthesized Cu_2O/AlZn-LDH composite elements uniformly, homogeneously, and completely cover the surface of the FTO electrode.

Electrochemical synthesis and behavior

Electrochemical deposition of AlZn-LDH could be achieved as follows. By applying negative potentials to the electrode, nitrate anions and zinc cations could be reduced on the FTO electrode. Since the reduction of zinc ions occurs at more negative potentials than the nitrate ions, in the presence of nitrate ions the reduction of zinc ions is not possible. The hydrogen evaluation reaction was also may be occurred. But at the used conditions for pH, mole ratio of Zn^{2+}/NO_3^- and the applied potential, only reduction of nitrate was occurred.[37] It should also be noted that at high temperatures and more negative potentials, ZnO is electrodeposited on the electrode.[37] Thus, at room temperature and at the optimum conditions, AlZn-LDH is electrochemically deposited on the electrode by following possible mechanism.

$$NO_3^- + H_2O + 2e^- \rightarrow NO_2^- + 2OH^- \quad (3)$$

$$(1-x)Zn^{2+} + xAl^{3+} + xNO_3^- \xrightarrow{2OH^-} (Zn^{2+}_{(1-x)}Al^{3+}_x(OH)_2)^{x+}(NO_3^-)_x \quad (4)$$

Figure 5a shows the cyclic voltammogram of AlZn-LDH in the 0.1M KOH solution. This cyclic voltammogram shows the AlZn-LDH was formed on the electrode. By applying -0.5V on AlZn-LDH electrode, a thin layer of Cu_2O was formed on the modified electrode in the presence of 0.05M citric acid as chelating agent [39]. Figure 5b also shows the cyclic voltammogram of Cu_2O/AlZn-LDH in the same solution.

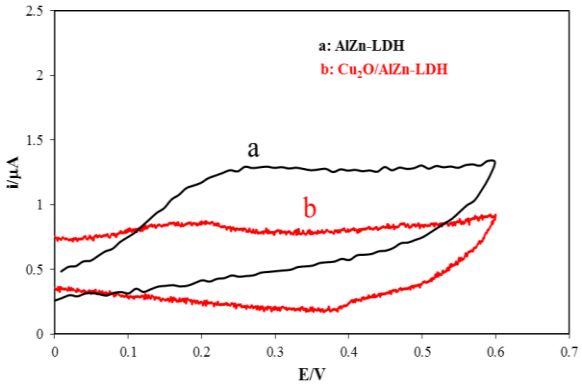

Figure 5. The cyclic voltammograms of (a) AlZn-LDH and (b) Cu_2O/AlZn/LDH modified FTO electrode in the 0.1 M KOH solution at the scan rate 50 mV s^{-1}.

Water oxidation

To evaluate the water oxidation activity of prepared materials, LSV curves were recorded with a scanning speed of 50 mv s^{-1} in 0.1 M KOH solution using the reference calomel electrode and platinum electrode as the counter electrode. The LSV voltammograms were reported in Figure 6. According to these data, it is clear that in comparison to Cu_2O, AlZn-LDH and Cu_2O/AlZn-LDH, the prepared composite (Cu_2O/AlZn-LDH) has a significant activity for the oxygen evaluation reaction. The onset potential for Cu_2O/AlZn-LDH was reported about 0.6 V vs. SCE, while onset potential at Cu_2O and AlZn-LDH were reported 0.75 and 1.25 respectively.

The current density of 10 mA/cm^2 was represented about 10% conversion efficiency at fuel systems using solar energy.[40, 41] So, it is important criteria at water oxidation that Cu_2O/AlZn-LDH needs an overpotential of about 380 mV to obtain the current density about 10 mA cm^{-2}, although, at Cu_2O and AlZn-LDH, the current density and catalytic activity were lower than that of Cu_2O/AlZn-LDH. Despite the low overpotentials, the Cu_2O/AlZn-LDH showed the highest current density at a certain applied potential. This result underscores the importance of assembling catalytically active materials at the molecular level when designing high performance electrochemical catalysts.[42]

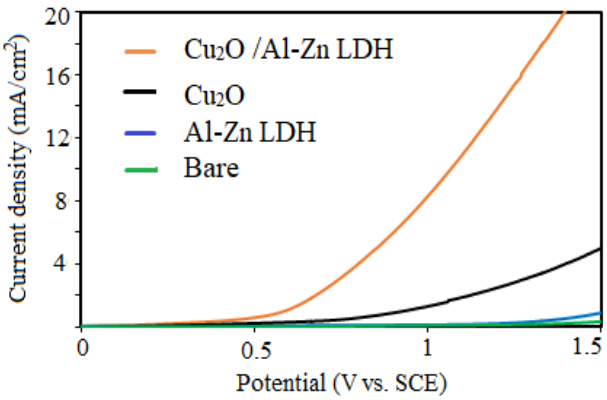

Figure 6. LSV curves of Cu_2O, AlZn-LDH and Cu_2O/AlZn-LDH.

Tafel slope, which describes the influence of potential or overpotential on the current density, is an important factor for the evaluation of OER kinetics. Tafel slope is often influenced by the electron and mass transport.[43] Tafel analysis of the OER on Cu_2O/AlZn-LDH and AlZn-LDH based electrocatalysts were conducted and the results are presented in Figure 7. within the electrocatalyst series, the Tafel slope increased in the following order: Cu_2O/AlZn-LDH (593 mV/dec) < AlZn-LDH (677 mV/dec). The small Tafel slope of Cu_2O/AlZn-LDH indicated that the electron and mass transfer easily occurred in Cu_2O/AlZn-LDH compared to AlZn-LDH. Therefore, the Tafel result supports the conclusion that the advanced electrocatalytic performance of Cu_2O/AlZn-LDH for OER was due to the presence of active sites (Al^{3+}, Cu^{2+}, and Al^{3+}) in Cu_2O/AlZn-LDH.

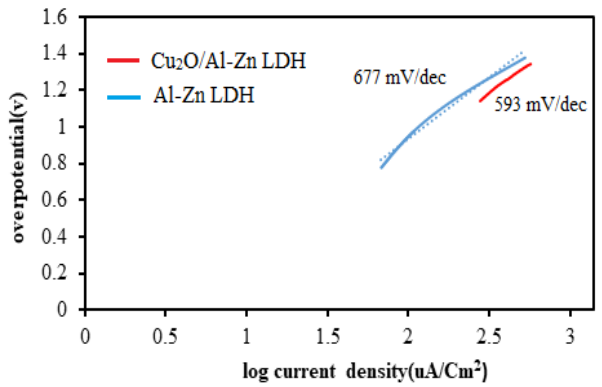

Figure 7. Tafel slop of Cu_2O/AlZn-LDH and AlZn-LDH.

The electrochemical stability of Cu_2O, AlZn-LDH, Cu_2O/AlZn-LDH electrodes were investigated by chronoamperometry in 0.1 M KOH solution. The chronoamperometry method expresses the time-dependent behavior and can report information on the durability of electrocatalyst through water oxidation reaction. As shown in Figure 8, the current densities remained constant for all three electrodes at constant overpotential within 50 s water oxidation. Therefore, the structures of AlZn-LDH, Cu_2O, Cu_2O/AlZn-LDH are stable in the water oxidation reaction. Also after 5 cycle chronoamperometry test, the stable current density with negligible degradation was observed, revealing their durability under water oxidation conditions.

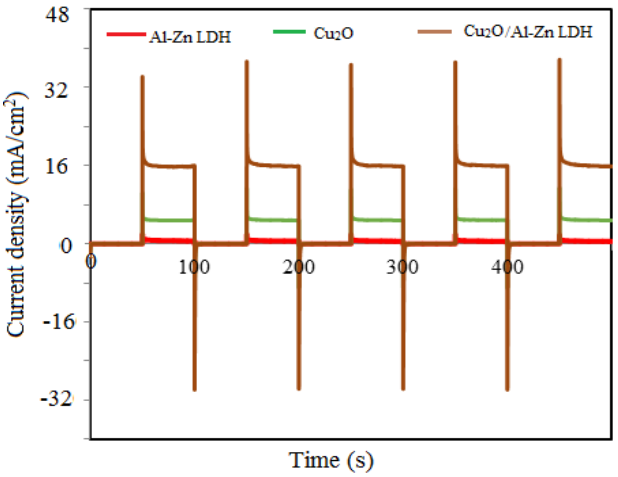

Figure 8. Chronoamperometry tests of AlZn-LDH, Cu_2O and Cu_2O/AlZn-LDH.

The electrochemical impedance method was used to investigate the resistance in electron transfer. Electrochemical impedance measurements for the FTO electrode and electrode modified with AlZn-LDH and Cu_2O/AlZn-LDH were studied using Nyquist diagrams and are shown in Figure 9. To study the charge transfer at the surface of the electrode, electrochemical impedance curves were recorded in the solution of 0.1 M $K_3[Fe(SCN)_6]$ and KCl for FTO and modified FTO. The diameter in this curve represents the charge transfer resistance between the electrode and the electrolyte. The diameter of the curve at modified electrodes is smaller than the bare electrode (FTO). This indicates that the modified electrodes have less resistance than the bare electrode.[44] Also, the diameter of Cu_2O and AlZn-LDH was larger than Cu_2O/AlZn-LDH. This indicates that the semiconductors Cu_2O/Al-Zn LDH have a higher conductivity than that of FTO, Cu_2O, and AlZn-LDH. These results were in agreement with the high oxygen evaluation reaction as shown in Figure 6.

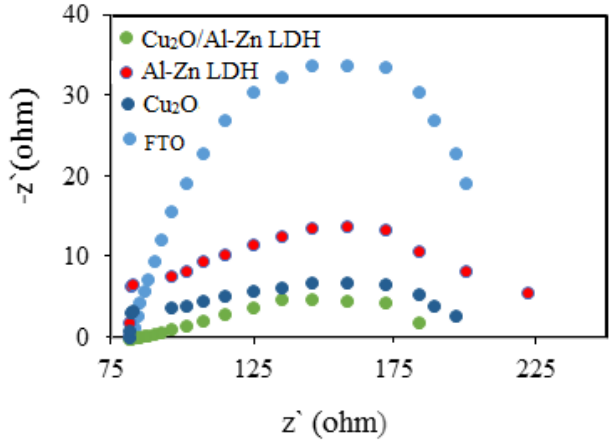

Figure 9. Electrochemical impedance measurements of AlZn-LDH, Cu_2O and Cu_2O/AlZn-LDH.

For the electrocatalytic OER over semiconductors, the possible mechanisms at alkaline solution have been reported. The reaction mechanism reported by Hunter et al. was as follows:[45]

$$4OH^- \rightarrow O_2\,(g) + 2H_2O\,(l) + 4e^- \quad (5)$$

$$4H_2O\,(l) + 4e^- \rightarrow 2H_2\,(g) + 4OH^- \quad (6)$$

$$2H_2O\,(l) \rightarrow O_2\,(g) + 2H_2\,(g) \quad (7)$$

Also, the electrocatalytic activity of Cu_2O/AlZn-LDH in comparison with the electrocatalysts reported in the literature, was summarized in Table 1.

Table 1. The electrocatalytic activity of Cu_2O/AlZn-LDH in comparison with the electrocatalysts reported in the literature

Electrocatalyst	Electrolyst	pH	Onset potential (V) SCE	Over potential at 10 mA cm^{-2}	Ref.
NiCu-LDH/SAV	1 M KOH	14	0.45	290	46
Cu@NiFe-LDH	1 M KOH	14	0.39	199	47
CC/Ni_2Cu-LDH	1 M KOH	14	0.44	370	48
Ni_2Cu-LDH	1 M KOH	14	0.54	770	48
Cu_2O/AlZn-LDH	0.1 M KOH	12	0.6	380	This study

4. CONCLUSIONS

The thin film Cu_2O/AlZn-LDH was successfully prepared on a FTO electrode using an easy, one-step electro-deposition method. This method can be applied for the synthesis of LDH based nanocomposite at a large scale. The obtained nanocomposite was characterized by different techniques. In this study, the electrochemical water oxidation activity of Cu_2O/AlZn-LDH was studied. The obtained results confirm that this nanocomposite can be used to the electrocatalytic water oxidation. The proposed Cu_2O/AlZn-LDH exhibited good water oxidation activity with the onset potential about 0.6 V vs. SCE and an overpotential of 380 mV at 10 mA cm^{-1}. The increased water oxidation activity of the Cu_2O/AlZn-LDH is attributed to a decrease in the charge transfer resistance which influences the electronic structure and consequently increases the electric conductivity and improves the water oxidation.

CONFLICTS OF INTEREST

There are no conflicts to declare.

AUTHOR INFORMATION

Corresponding Authors

Karim Asadpour-Zeynali: Email: k.zeynali@gmail.com,
ORCID: 0000-0001-9820-552X
Kamellia Nejati: Email: nejati_k@yahoo.com,
ORCID: 0000-0002-7716-7971

Author(s)

Parisa Beikzadeh, Leila Jafari Foruzin

ACKNOWLEDGEMENTS

The authors are gratefully acknowledged the University of Tabriz for financial support.

REFERENCES

1. P. W. Menezes, A. Indra, C. Das, C. Walter, C. Göbel, V. Gutkin, D. Schmeiβer, M. Driess, *ACS Catal*., **2017**, *7*, 103-109.
2. Y. Hou, M. Qiu, T. Zhang, J. Ma, S. Liu, X. Zhuang, C. Yuan, X. Feng, *Adv. Mat*. **2017**, *29*, 1604480.
3. S. Y. Ryu, M. R. Hoffmann, *Catalysts*, **2016**, *6*, 59-74.
4. X. Li, X. Hao, A. Abudula, G. Guan, *J. Mater. Chem*., **2016**, *4*, 11973-12000.
5. T. Reier, Z. Pawolek, S. Cherevko, M. Bruns, T. Jones, D. Teschner, S. R. Selve, A. Bergmann, H. N. Nong, R. Schlögl, *J. Am. Chem. Soc.*, **2015**, *137*, 13031-13040.
6. S. Liu, L. Li, H. S. Ahn, A. Manthiram, *J. Mater. Chem.*, **2015**, *3*, 11615-11623.
7. P. Li, R. Ma, Y. Zhou, Y. Chen, Z. Zhou, G. Liu, Q. Liu, G. Peng, Z. Liang, J. Wang, *J. Mater. Chem.*, **2015**, *3*, 15598-15606.
8. G. S. Hutchings, Y. Zhang, J. Li, B. T. Yonemoto, X. Zhou, K. Zhu, F. Jiao, *J. Am. Chem. Soc*., **2015**, *137*, 4223-4229.
9. L. Wu, Q. Li, C. H. Wu, H. Zhu, A. Mendoza-Garcia, B. Shen, J. Guo, S. Sun, *J. Am. Chem. Soc*., **2015**, *137*, 7071-7074.
10. G. He, W. Zhang, Y. Deng, C. Zhong, W. Hu, X. Han, *Catalysts*., **2017**, *7*, 366-383.
11. M. K. Bates, Q. Jia, H. Doan, W. Liang, S. Mukerjee, *ACS Catal*., **2016**, *6*, 155-161.
12. B. Weng, F. Xu, C. Wang, W. Meng, C. R. Grice, Y. Yan, *Energy Environ. Sci*., **2017**, *10*, 121-128.
13. X. Han, Y. Yu, Y. Huang, D. Liu, B. Zhang, *ACS Catal.*, **2017**, *7*, 6464-6470.
14. L. Zhou, M. Shao, J. Li, S. Jiang, M. Wei, X. Duan, *Nano Energy*, **2017**, *41*, 583-590.
15. G. Zhang, G. Wang, Y. Liu, H. Liu, J. Qu, J. Li, *J. Am. Chem. Soc*., **2016**, *138*, 14686-14693.
16. Y. Tan, H. Wang, P. Liu, Y. Shen, C. Cheng, A. Hirata, T. Fujita, Z. Tang, M. Chen, *Energy Environ. Sci*., **2016**, *9*, 2257-2261.
17. W. Li, S. Zhang, Q. Fan, F. Zhang, S. Xu, *Nanoscale*, **2017**, *9*, 5677-5685.
18. F. Lu, M. Zhou, Y. Zhou, X. Zeng, *Small*, **2017**, *13*, 1701931-1701949.
19. M. B. Stevens, L. J. Enman, A. S. Batchellor, M. R. Cosby, A. E. Vise, C. D. Trang, S. W. Boettcher, *Chem. Mater*., **2017**, *29*, 120-140.
20. D. -C. Xia, L. Zhou, S. Qiao, Y. Zhang, D. Tang, J. Liu, H. Huang, Y. Liu, Z. Kang, *Mater. Res. Bull*., **2016**, *74*, 441-446.
21. J. Jiang, A. Zhang, L. Li, L. Ai, *J. Power Sources*, **2015**, *278*, 445-451.
22. X. Yu, M. Zhang, W. Yuan, G. Shi, *J. Mater. Chem.*, **2015**, *3*, 6921-6928.
23. X. Long, J. Li, S. Xiao, K. Yan, Z. Wang, H. Chen, S. Yang, *Angew. Chem.*, **2014**, *126*, 7714-7718.
24. W. Huang, H. Zhong, D. Li, P. Tang, Y. Feng, *Electrochim. Acta*, **2015**, *173*, 575-580.
25. D. Tang, Y. Han, W. Ji, S. Qiao, X. Zhou, R. Liu, X. Han, H. Huang, Y. Liu, Z. Kang, *Dalton Trans.*, **2014**, *43*, 15119-15125.
26. J. Ping, Y. Wang, Q. Lu, B. Chen, J. Chen, Y. Huang, Q. Ma, C. Tan, J. Yang, X. Cao, *Adv. Mater*., **2016**, *28*, 7640-7645.
27. J. Suntivich, K. J. May, H. A. Gasteiger, J. B. Goodenough, Y. Shao-Horn, *Science*, **2011**, *334*, 1383-1385.
28. S. Anantharaj, K. Karthick, S. Kundu, *Mater. Today Energy*, **2017**, *6*, 1-26.
29. S. J. Kim, Y. Lee, D. K. Lee, J. W. Lee, J. K. Kang, *J. Mater. Chem*., **2014**, *2*, 4136-4139.

30. T. Wang, X. Zhang, X. Zhu, Q. Liu, S. Lu, A. M. Asiri, Y. Luo, X. Sun, *Nanoscale*, **2020**, *12*, 5359-5362.
31. M. Gong, H. Dai, *Nano Res*., **2015**, *8*, 23-39.
32. M. Shao, R. Zhang, Z. Li, M. Wei, D. G. Evans, X. Duan, *Chem. Commun*., **2015**, *51*, 15880-15893.
33. F. Dionigi, P. Strasser, *Adv. Energy Mater*., **2016**, *6*, 1600621-1600641.
34. M. S. Burke, L. J. Enman, A. S. Batchellor, S. Zou, S. W. Boettcher, *Chem. Mater*., **2015**, *27*, 7549-7558.
35. K. Nejati, K. Asadpour-Zeynali, *Mater. Sci. Eng.*, **2014**, *35*, 179-184.
36. K. Nejati, S. Davari, A. Akbari, K. Asadpour-Zeynali, Z. Rezvani, *Int. J. Hydrogen Energy*, **2019**, *44*, 14842-14852.
37. M. S. Yarger, E. M. Steinmiller, K. -S. Choi, *Inorg. Chem*., **2008**, *47*, 5859-5865.
38. L. Pan, Y. Liu, L. Yao, D. Ren, K. Sivula, M. Grätzel, A. Hagfeldt, *Nature Commun*., **2020**, *11*, 1-10.
39. H. Lahmar, F. Setifi, A. Azizi, G. Schmerber, A. Dinia, *J. Alloys Compd.*, **2017**, *718*, 36-45.
40. L. -J. Zhou, X. Huang, H. Chen, P. Jin, G.-D. Li, X. Zou, *Dalton Trans*., **2015**, *44*, 11592-11600.
41. C. C. L. McCrory, S. Jung, J. C. Peters, T. F. Jaramillo, *J. Am. Chem. Soc*., **2013**, *135*, 16977-16987.
42. L. J. Foruzin, B. Habibi, Z. Rezvani, *New J. Chem*., **2018**, *42*, 13963-13970.
43. Z. Lu, L. Qian, Y. Tian, Y. Li, X. Sun, X. Duan, *Chem. Commun*., **2016**, *52*, 908-911.
44. K. Nejati, L. J. Foruzin, Z. Rezvani, *Dalton Trans.*, **2021**, *50*, 7223-7228.
45. B. M. Hunter, H. B. Gray, A. M. Müller, *Chem. Rev*., **2016**, *116*, 14120-14136.
46. Y. -S. Xie, Z. Wang, M. Ju, X. Long, S. Yang, *Chem. Sci.*, **2019**, *10*, 8354-8359.
47. L. Yu, H. Zhou, J. Sun, F. Qin, F. Yu, J. Bao, Y. Yu, S. Chen, Z. Ren, *Energy Environ. Sci*., **2017**, *10*, 1820-1827.
48. Y. Zheng, J. Qiao, J. Yuan, J. Shen, A. -J. Wang, P. Gong, X. Weng, L. Niu, *Electrochim. Acta*, **2018**, *282*, 735-742.